九州大学学術情報リポジトリ
Kyushu University Institutional Repository

Enhancement of Photocatalytic Properties of Carbon Dot Supported by AgNPs for Methylene Blue Degradation

Kusumandari, Kusumandari
Department of Physics, Faculty of Mathematics and Natural Sciences, Sebelas Maret University

Riski Intan Prasasti
Department of Physics, Faculty of Mathematics and Natural Sciences, Sebelas Maret University

Isnaeni, Isnaeni
Research Center for Physics, National Research and Innovation Agency,

https://doi.org/10.5109/7236852

出版情報：Evergreen. 11 (3), pp.2071-2080, 2024-09. 九州大学グリーンテクノロジー研究教育センター
バージョン：
権利関係：Creative Commons Attribution 4.0 International

Enhancement of Photocatalytic Properties of Carbon Dot Supported by AgNPs for Methylene Blue Degradation

Kusumandari Kusumandari[1,*], Riski Intan Prasasti[1], Isnaeni Isnaeni[2]

[1]Department of Physics, Faculty of Mathematics and Natural Sciences, Sebelas Maret University, Central Java, Indonesia

[2]Research Center for Physics, National Research and Innovation Agency, South Tangerang, Indonesia

*Author to whom correspondence should be addressed:
Email: kusumandari@staff.uns.ac.id

(Received October 28, 2023: Revised March 14, 2024: Accepted June 21, 2024).

Abstract: Efforts to degrade liquid waste have been carried out, one of which is using photocatalyst materials. In this work, Carbon Dots (CDs) in combination with silver nanoparticles (AgNPs) were used to degrade methylene blue (MB). CDs were synthesized from urea with added citric acid using a bottom-up microwave method. While AgNPs were synthesized from silver plates using the Nd:YAG laser ablation method. The absorbance and the fluorescence spectra of CDs were observed via a UV-Vis and a 405 nm laser photoluminescence (PL) spectrophotometer, respectively. Fourier Transform Infrared (FTIR) was employed to study the CDs functional group. Meanwhile, the particle size of CDs and AgNPs was measured using Transmission Electron Microscopy (TEM). In order to observe the photocatalytic performance, CDs with various concentrations of AgNPs were dissolved in the MB solution. The influences of AgNPs on the photocatalytic performance of CDs were examined using a UV-Vis spectrophotometer. As a result, CDs with a concentration of 2 ppm were the most optimal as a catalyst with a degradation percentage of 88.8%. Moreover, adding one ppm AgNPs increased the photocatalytic activity to 93.4%.

Keywords: photocatalyst; CDs; AgNPs; methylene blue; degradation

1. Introduction

Liquid waste resulting from textile industry activities contains many highly toxic dyes. Untreated disposal is harmful to the environment and threatens aquatic life[1,2]. Concerns about the high level of environmental pollution have led to increased research to find treatment methods with sustainable, cost-effective, and environmentally friendly strategies[3]. Commonly, organic and inorganic contaminants in wastewater were treated using physical, biological, and chemical methods[4-7].

The photodegradation method is effective in considering the balance between efficiency and cost[8]. This process uses a catalyst and ultraviolet (UV) irradiation. Photodegradation using UV-C light is reported to achieve better degradation than UV-A because of its incredible energy to excite the catalyst[9].

Carbon-based materials are broadly utilized as metal-free catalysts or bolsters in energy[10], catalysis process[11,12,13], and environmental applications[14,15] because of their interesting properties. One of the carbon-based materials is carbon dots (CDs). It offers advantages in terms of excellent optical properties and photostability. It is also easy to fabricate with negligible toxicity and cost. CDs can be applied in technological advances such as biosensors, LEDs, drug delivery, biological imaging, and photocatalysis[16]. The surface of CDs has abundant functional groups with excellent photoelectric properties, namely electron transfer and storage capacity, photoluminescence, and broad optical[17]. Moreover, CDs can be greenly synthesized from renewable raw materials such as leaves, flowers, roots, and other biomass. It also can be synthesized from renewable refined compounds such as urea, citric acid, amino acids, *etc*[18]. These materials are very eco-friendly and can be obtained easily at low prices. So, this is an added value for carbon dots. Generally, CDs can be fabricated via two main methods: bottom-up or top-down. The top-down process includes laser ablation, electrochemical oxidation of graphite, and chemical oxidation of activated carbon. Meanwhile, the bottom-up processes consist of hydrothermal, ultrasonication, and microwave processes[19]. Among them, the microwave method is proposed as an alternative to the conventional hydrothermal method because of the shorter synthesis time and less energy consumption[20]. Sendão *et al*. compare making CDs using hydrothermal and microwave methods[21]. The hydrothermal method takes 2-4 hours, while the microwave method only takes 5-10 minutes.

Concerning CDs as catalyst materials, Jusuf *et al.* use

CDs as a single catalyst and succeeded in degrading dyes up to 90% under sunlight irradiation for 10 hours[22]. Here, the time required is still too long and needs to be reduced by enhancing the photocatalytic activity of CDs combined with other materials. Combining several materials with mutually supportive properties is believed to improve photocatalytic activity. For example, Gan *et al.* prepared CDs nanocomposites with precious metals to advance photocatalytic performance[23]. The photocatalytic effect is enhanced by transferring electrons from the CDs to the metal and vice versa. Silver nanoparticles (AgNPs) are precious metal materials that exhibit Surface Plasmonic Resonance (SPR) properties. This property can be used to widen the range of light absorption[17]. Commonly, CDs and AgNPs are made of composite materials. However, this requires a complex fabrication process and involves toxic reducing agents such as sodium borohydride[24]. It would be interesting to synthesize CDs and enhance this photocatalytic activity using AgNPs in a friendly method.

In this work, the CDs fabrication from citric acid and urea via microwave technique as a photocatalytic application was performed. AgNPs were added to CDs in the colloidal phase as a mixed catalyst without adding other chemicals. Moreover, the effect of AgNPs on CDs as a catalyst in degrading methylene blue (MB) dye was observed.

2. Materials and methods

2.1 Materials

Urea and citric acid were used as materials sources of CDs While silver plate was used as a source of AgNPs synthesis. Methylene blue (MB) dissolved in the aqua bides with 1 ppm concentration was used as a pollutant solution model.

2.2 Synthesis of CDs

CDs were made from urea, and citric acid was added via a bottom-up microwave method. A total of 2 grams of urea and citric acid were diluted in 40 ml of distilled water. Afterward, it was homogenized for 5 minutes using a magnetic stirrer at 250 rpm. Next, it was heated in a microwave at 800W for 4-5 minutes. As a result, the dark brown crust was obtained. The crust was liquified in 20 ml of distilled water to form CDs solution. Then, it was visually tested using a UV laser with an excitation wavelength of 405 nm to determine whether the CDs were successfully synthesized. When it works, CDs fluoresce in the visible light range. By dilution method, CDs were made in various concentrations of 2, 4, 8, and 16 ppm.

2.3 Synthesis of AgNPs

AgNPs were synthesized using the Nd:YAG laser ablation method. Laser setup with a wavelength of 1064 nm, power 100 mW. A 10-15 ml of Aquabides was prepared. The silver plate, measured by mass, is placed in a beaker and positioned precisely in the laser beam. The laser is turned on, and the beaker is rotated to distribute the laser beam evenly onto the silver plate. The process lasts for 3 minutes. The steps were repeated until a sufficient stock of AgNPs solution was obtained. When the process is complete, the mass of the silver plate is measured again to determine the mass of dissolved silver. The AgNPs that had been successfully synthesized were then made in four different concentrations of 1, 2, 4, and 8 ppm by dilution method.

2.4 Instruments

The absorbance of CDs and AgNPs was examined through a UV-Vis Ocean Optic spectrophotometer MAYA 2000 at wavelengths of 200 – 800 nm. The fluorescence spectra of CDs were measured using a photoluminescence (PL) spectrophotometer with a 405 nm laser as the excitation source. The function groups of CDs were measured at wavenumbers of 400 – 4000 cm^{-1} by FTIR spectrophotometer. The particle size of CDs and AgNPs was measured via the Transmission Electron Microscopy (TEM) method.

2.5 Photocatalytic Performance

The photocatalytic performance was tested under UV-C irradiation for 4x30 minutes. The first experiment used a single CDs catalyst with variations in concentration, then the results were analyzed. The volume ratio of CDs and MB dye was 1 ml: 10 ml. Then, the most optimal concentration of CDs will be used in the following experiment. The CDs and AgNPs catalysts each had a volume of 1 ml and were mixed in the colloidal phase before being used to degrade MB dye. The observed photocatalytic activity in the form of degradation percentage and kinetics rate were calculated by equations (1) and (2):

$$\%D = \left[\frac{C_0 - C_t}{C_0}\right] \times 100\% \quad (1)$$

$$\ln\frac{c_0}{c_t} = kt \quad (2)$$

C_0 is the initial absorbance, C_t is the absorbance after the t time, k is kinetic reaction rate, t is the time, and %D is the degradation percentage.

3. Results and discussion

3.1 Optical Properties of CDs

When the CDs colloid was irradiated by a UV laser with a wavelength of 405 nm, a green glow was emitted, as demonstrated by Fig. 1. This indicates that CDs have formed [22,25]. Emissions arise because electrons absorb energy from UV light which causes electron excitation to

the conduction band and leaves holes in the valence band. In this unstable state, the electron will recombine, accompanied by the release of electromagnetic wave luminescence or fluorescence[26].

Figure 2 shows the spectra of absorbance and photoluminescence of CDs with various concentrations. The intensity of the absorbance will be higher as the concentration increases, as presented in Fig. 2(a). Each sample has two absorbance peaks at around 345 and 230 nm. It is known that the CDs have surface transitions of C=O bonds at wavelengths of 342, 339, 338, and 337 nm, respectively[27]. Also, core transitions of CDs appear as C=C bonds at wavelengths 234, 225, 246, and 243 nm[28].

The peaks of photoluminescence for concentrations of 2, 4, 8, and 16 ppm were obtained at wavelengths 531 and 529 nm, respectively, corresponding to the green color[29], as revealed in Fig. 2(b).

Fig 1. Fluorescence of CDs

Figure 2(c) shows the bandgap energy of the CDs analyzed using the Tauc Plot method. An average bandgap value of 3.28 eV was obtained. This result is in accordance with previous research (around 1.5 - 3.5 eV[30].

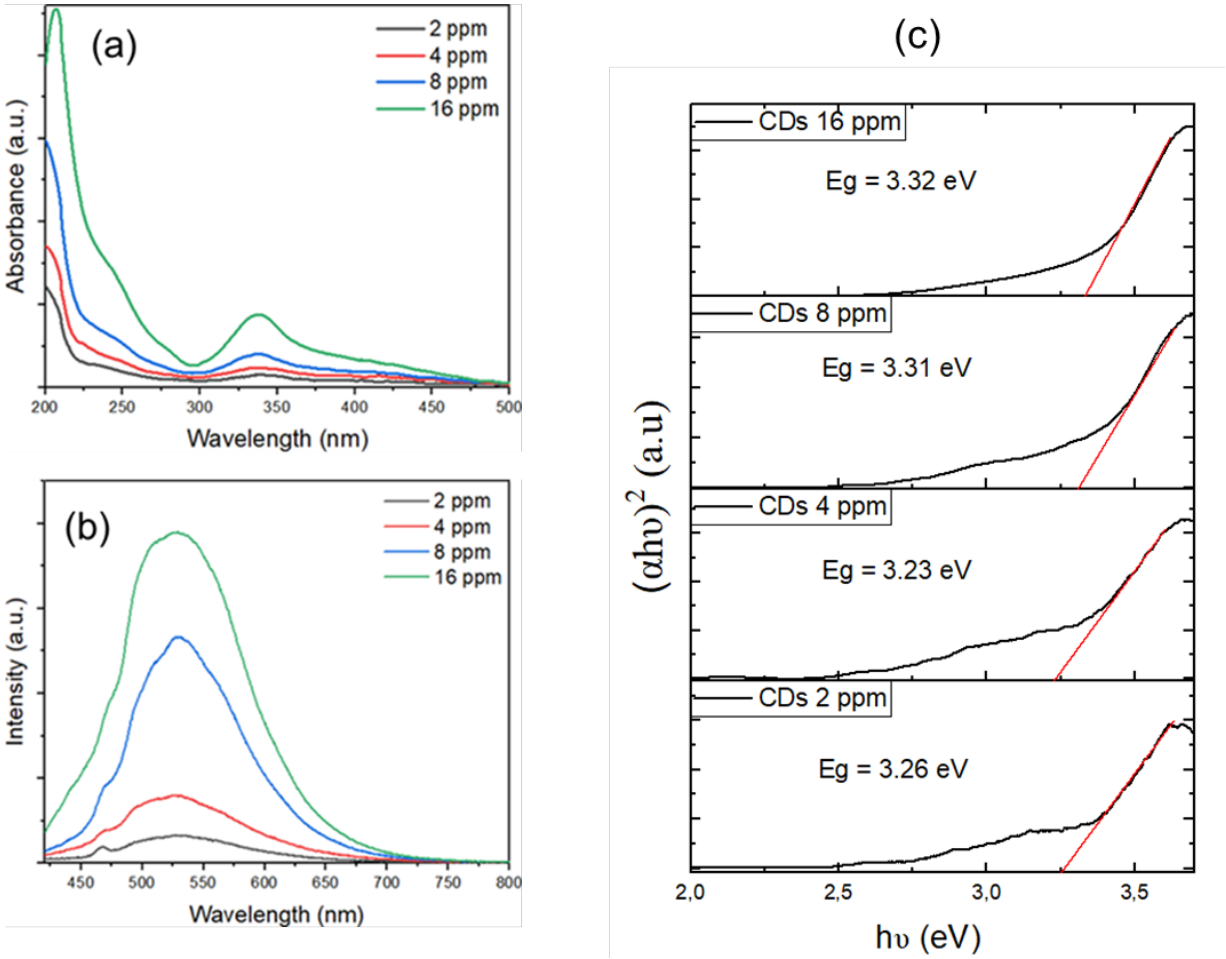

Fig 2. Optical properties of CDs: (a) absorbance, (b) photoluminense, and (c) bandgap energy (Eg) of CDs at concentrations of 2, 4, 8, and 16 ppm

3.2 Particle size and functional groups of CDs

Figure 3 shows a TEM image of CDs sample. The observed particle image is black spherical, as demonstrated by Fig. 3(a). Moreover, Fig.3(b) reveals the measurement of 34 CDs particles whose average size was 3.2 nm. This result agrees with others that the CDs nanoparticle size is less than 10 nm[31]. The FTIR characterization of the CDs samples is presented in Fig. 4.

The broadband transmittance at 3322 cm^{-1} indicates the stretching of the O-H group. The sharp transmittance at 1634 cm^{-1} is the vibration of C=O originating from the aromatic carbonyl functional group[32]. The peak at 2132 cm^{-1} indicates the C-H stretching. Meanwhile, the peak of 1469 cm^{-1} relates to the C-O stretching vibrations. Also, the peak at 1287 cm^{-1} indicates C-N groups[16].

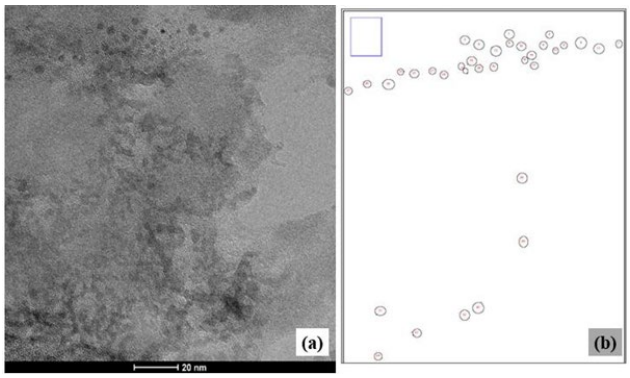

Fig 3. (a) TEM image and (b) particle size of CDs

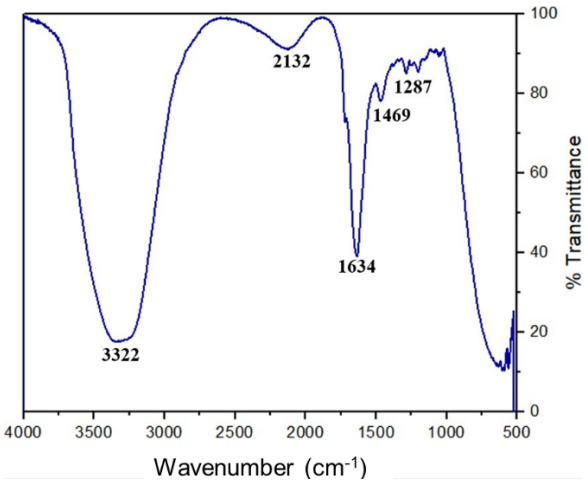

Figure 4. Functional group of CDs

3.3 The AgNPs characterization

The AgNPs were synthesized from a pure silver plate using laser ablation. Physically, the solution changes from a clear solution to a brownish-yellow solution indicating AgNPs formation. Figure 5 shows the TEM image of AgNPs sized 23.3 nm on average, in the 6.5 - 53.6 nm range. These results indicate that AgNPs have been successfully produced since they have a size below 100 nm. It is agreed with the previous report which synthesized AgNPs from the same source[33].

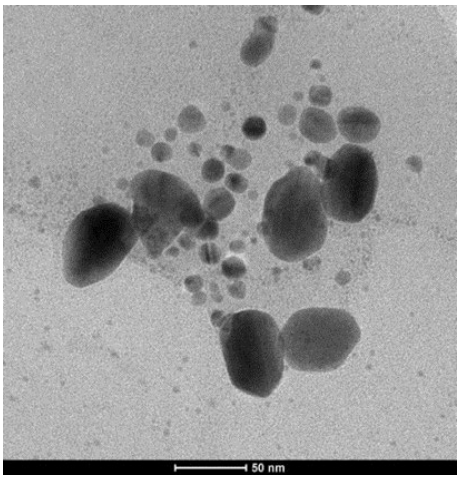

Fig 5. TEM image of AgNPs

Figure 6 shows the absorbance spectra of AgNPs with concentrations of 1, 2, 4, and 8 ppm. The resulting peaks are in almost the same wavelength, namely in the 401-405 nm range. This absorbance peak is the occurrence of the SPR phenomenon. This result agrees with the previous study that the absorbance peak of silver nanoparticles synthesized from pure silver chips was at a wavelength of 420 nm[33].

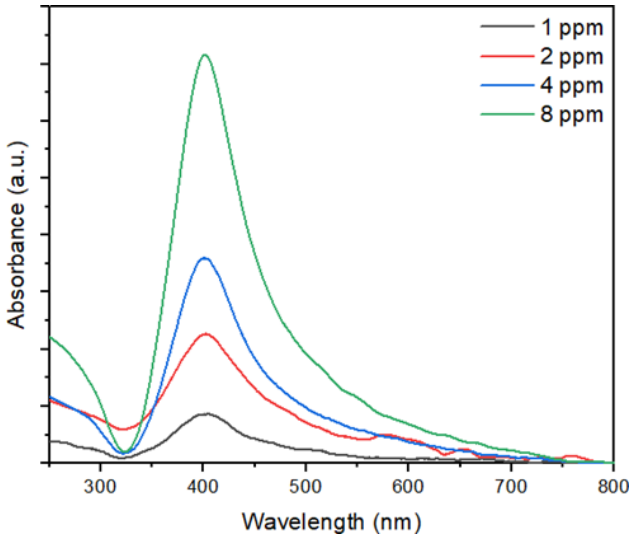

Fig 6. Absorbance spectra of AgNPs

Figure 7 shows the bandgap energy of AgNPs. An average bandgap value of 2.73 eV was obtained. This result is almost the same as the previous one obtained by Zewudie *et al*. [34]

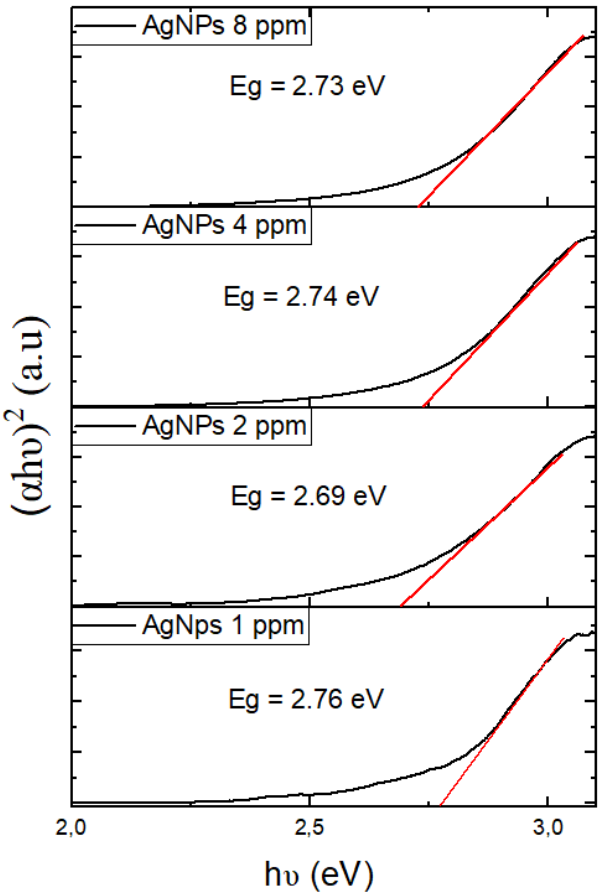

Fig 7. Bandgap energy (Eg) of AgNPs at 1, 2, 4, and 8 ppm concentrations.

3.4 Methylene blue degradation with CDs

Colloidal CDs were used as a catalyst to degrade MB dye using UV-C irradiation for 2 hours, as exhibited in Fig. 8. Figure 8(a) shows that MB degradation increases with increasing irradiation time. The percentage of degradation is calculated using equation (1). In the MB dye irradiation without CDs, the degradation percentage was 80.46%. This degradation occurs because UV-C light is also contributing to photodegradation. The reaction process is shown in equation (3). When the MB dye reacts with oxygen and gets energy or photons from UV-C light, it will break the bond. The molecule will decompose into salt, water, and carbon dioxide gas [35].

$$C_{16}H_{18}N_3SCl + 25{,}5O_2 + hv \rightarrow HCl + H_2SO_4 + 3HNO_3 + 16CO_2 + 6H_2O \quad (3)$$

The addition of the CDs catalyst with various concentrations of 2, 4, 8, and 16 ppm resulted in the percentage degradation of MB of 88.8%, 79%, 77.3%, and 77.3%. The greatest degradation percentage was carried out on CDs with a concentration of 2 ppm. The kinetics reaction rate (k) was calculated using equation (2). The gradient value shows the magnitude of the degradation rate, namely 0.0135/minute, 0.0185/minute, 0.0121/minute, 0.0121/minute, and 0.0122/minute for the concentrations of CDs 0, 2, 4, 8, and 16 ppm, respectively, as demonstrated in Fig. 8(b). Adding a CDs catalyst with a concentration of 2 ppm increased the effectiveness of the degradation by 8.34% compared to without, as shown in Fig. 8(c). Catalysts play an essential role in separating electrons and holes to produce radicals that react with pollutants. A schematic of the mechanism of photocatalysis using CDs is shown in Fig. 8(d). Photocatalytic activity occurs when photons or UV-C light with energy equal to or more than the CDs band gap are absorbed by CDs particles. This energy absorption will excite electrons of the CDs material to the conduction band and leave a hole (h+) in the valence band. Then, the electrons will carry out a reduction reaction with O_2 to form superoxide anion radicals ($O-$). The electrons also react with O_2 and H_2O to produce H_2O_2. On the other hand, holes carry out oxidation reactions with H_2O to produce free radicals OH* [36]. The photodegradation reaction using a CDs catalyst follows the equation below (4-10):

$$CDs + hv \rightarrow e^- + h^+ \quad (4)$$
$$e^- + O_2 \rightarrow O^{-2} \quad (5)$$
$$2e^- + H_2O + O_2 \rightarrow H_2O_2 \quad (6)$$
$$O_2^- + methylene\ blue \rightarrow color\ reduction \quad (7)$$
$$H_2O_2 + methylene\ blue \rightarrow H_2O + CO_2 \quad (8)$$
$$h^+ + H_2O \rightarrow OH^* \quad (9)$$
$$OH^* + methylene\ blue \rightarrow oxidation \quad (10)$$

It is seen that the more free radicals formed resulted in a faster MB degradation process. The reaction in equations (4) to (10) shows that the CDs catalyst can degrade MB dyes, resulting in H_2O and CO_2 gas that evaporates into the air and other compounds in the form of several acids that have no color[36]. However, adding more catalysts lowers the percentage of degradation. This is because the greater the concentration of CDs, the more molecules. When added to MB dye, CDs with high concentrations will overlap among CDs particles or aggregation occurs. It will prevent light's energy from reacting with the surface of CDs particles that are in contact with the MB. In addition, there is too much aggregation of CDs particles, thereby reducing the active surface of CDs as illustrated in Fig. 8(e).

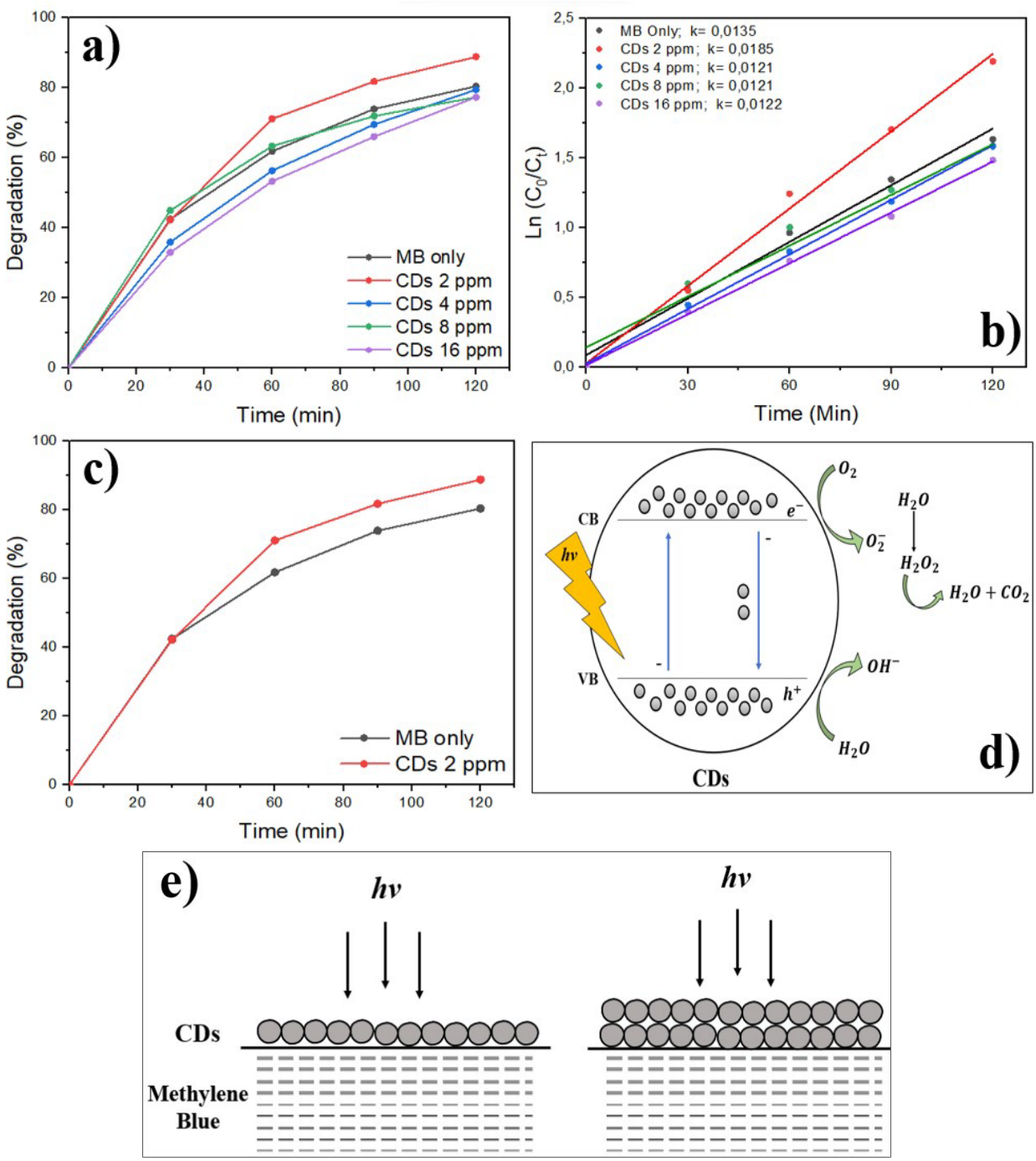

Fig 8. Photocatalytic activity of CDs (a) percentage of degradation, (b) rate of kinetics reaction, (c) comparison of degradation between MB without and with CDs 2 ppm, (d) schematic of the photocatalytic mechanism, (e) illustration of the high concentration of CDs.

3.5 MB degradation with CDs and AgNPs

The AgNPs with 1, 2, 4, and 8 ppm concentrations are used as admixtures in CDs 2 ppm for catalysts. Figure 9(a) shows the percentage of MB degradation without, with CDs 2 ppm and CDs 2 ppm/AgNPs catalyst at various time irradiation. For 120 min of irradiation, the percentage of MB degradation using CDs (2 ppm) and AgNPs 1, 2, 4, 6, and 8 ppm is 93.4%, 88.6%, 88.7%, and 87.5%, respectively. The highest photodegradation activity was obtained for the sample of CDs 2 ppm and AgNPs 1 ppm. The kinetics rates obtained were 0.0657/min, 0.0169/min, 0.0149/min, and 0.207/min, as shown in Fig. 9(b). Compared to a single CDs catalyst, adding AgNPs to CDs enhanced the photocatalytic activity of MB dye by up to 4.6%.

The possible mechanism of photocatalyst using a mixture of CDs and AgNPs is illustrated in Fig. 9(c).

Electrons on CDs will easily move to the surface of AgNPs and vice versa. Moreover, the photoelectric properties of CDs can enhance electron-hole pair separation. Furthermore, as an effect of strong SPR, AgNPs are also stimulated to reduce electron-hole pair recombination, thereby increasing catalytic activity. Then, the electrons will move to the surface and react with O_2, resulting in radicals as agents to degrade the pollutant. These aspects are the reason for the enlarged photocatalytic properties of CDs mixed with AgNPs[17,37]. Also, the light absorbance range becomes wider with the addition of AgNPs since CDs have strong absorbance in the far UV and AgNPs in the near UV, as shown in Fig. 2(a) and 6. Jing et al. investigated the mechanism of electron transfer and photodegradation process on g-C_3N_4 dots/graphene system using density functional theory calculation. The study concluded that g-C_3N_4 dots/graphene is better in terms of photo adsorption/electron-hole generation, lower electron recombination and higher free radical producing than g-C_3N_4 dots alone[38]. The same mechanism may also apply to the mixture of CDs and AgNPs in this study.

However, if the AgNPs content is excessive, it can reduce the degradation. Several possible reasons may cause a decrease in photocatalytic activity. First, the large number of AgNPs molecules can block photon energy from light to reach the surface of CDs and other AgNP particles in direct contact with MB dye. So that there is no separation of electron-hole pairs and redox reactions. Second, AgNPs combine or aggregate, reducing the active surface of AgNPs and CDs molecules. Third, AgNPs may act as recombination centers due to the electrostatic attraction of positive Ag to negative electrons. Therefore, optimizing the number of AgNPs that should be added is also a challenge.

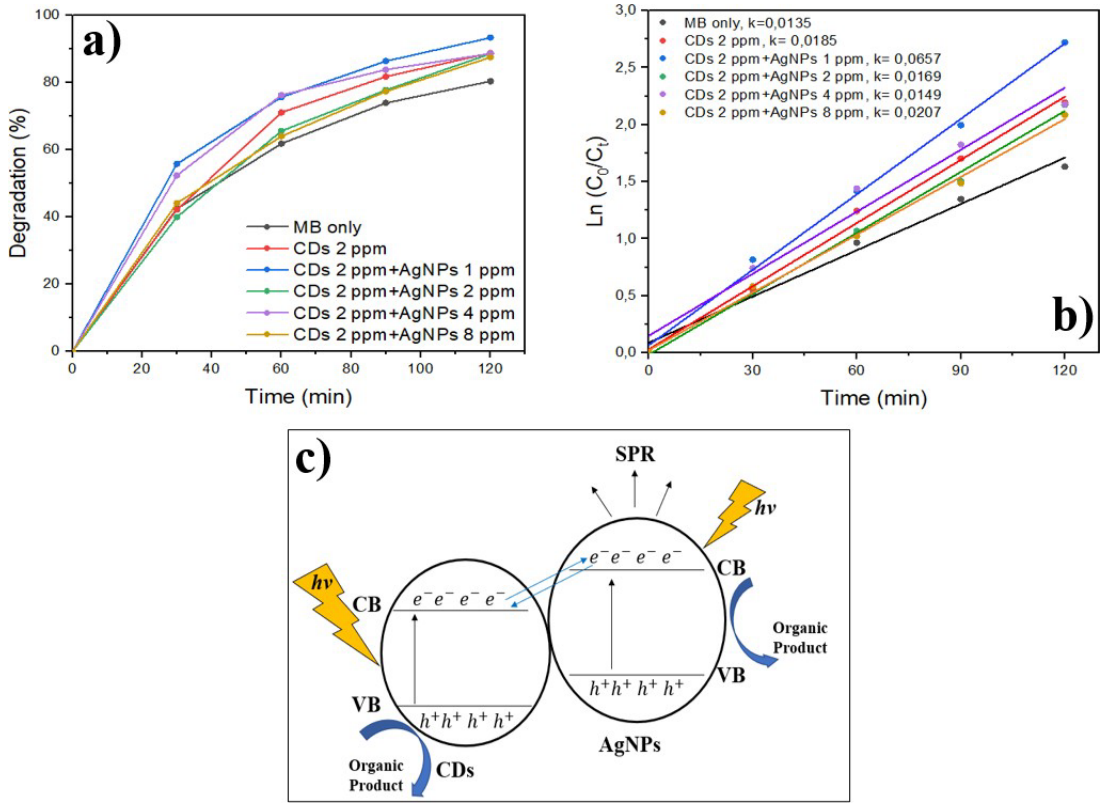

Fig 9. Results of photocatalytic activity of CDs mixed with AgNPs, (a) percentage of degradation, (b) rate of degradation, (c) mechanism of photocatalysis.

4 Conclusion

The CDs from citric acid and urea was successfully synthesized within 4-5 minutes under microwave irradiation. The AgNPs were successfully synthesized using the laser ablation method. Variations in the concentration of CDs were used to apply MB dye degradation under UV-C irradiation. The CDs with 2 ppm of concentration resulted in a degradation percentage of 88.8%. Adding 1 ppm AgNPs increased the degradation activity to 93.4%. However, increasing the concentration of CDs and AgNPs that are too much is not beneficial because it prevents the formation of electron-hole pairs and reduces free-radicals formation as degrading agents. In addition, it also reduces the active surface due to aggregation. However, this is economically beneficial because it only requires a small catalyst concentration for the degradation process.

Acknowledgement

The authors would like to thank the Directorate General of Higher Education, Research, and Technology, Republic of Indonesia, for supporting this research.

References

1) I. Fatimah, I. Sahroni, M. S. E. Dahlyani, A. M. N. Oktaviyani, and R. Nurillahi, "Surfactant-modified Salacca zalacca skin as adsorbent for removal of methylene blue and Batik's wastewater," *Materials Today: Proceedings*, **44**, 3211-3216 (2021), DOI: 10.1016/j.matpr.2020.11.440.
2) S. Samsami, M. Mohamadizaniani, M. H. Sarrafzadeh, E. R. Rene, and M. Firoozbahr, "Recent advances in the treatment of dye-containing wastewater from textile industries: Overview and perspectives," *Process safety and environmental protection*, **143**, 138-163 (2020), DOI: 10.1016/j.psep.2020.05.034.
3) A. L. Chang, B. S. Nguyen, V. H. Nguyen, and C. Hu, "Adsorption kinetics of methyl blue using metal-modified barium lanthanum titanate as an effective absorbent," *Materials Chemistry and Physics*, **276**, 125363 (2022), DOI: 10.1016/j.matchemphys.2021.125363.
4) A.D. Ghaisani, A. Mahayum, K. Kusumandari, and T.E. Saraswati, "Degradation of dyes in textile industry wastewater using dielectric barrier discharge (DBD) plasma," *AIP Conference Proceedings*, **2097**, 030097 (2019). DOI:10.1063/1.5098272
5) K. Kusumandari, T.E. Saraswati, S.W. Wulandari, and A. Qusnudin, "Atmospheric air plasma corona discharge for dye degradation of Indonesian batik wastewater," *Indian J Phys*, **96**, 1001–1008 (2022). DOI:10.1007/s12648-021-02082-5.
6) M.S.A Ja'farawy, K. Kusumandari, A. Purwanto, and H. Widiyandari, "Carbon quantum dots supported zinc oxide (ZnO/CQDs) efficient photocatalyst for organic pollutant degradation – A systematic review," *Environmental Nanotechnology, Monitoring & Management,* **18**, 100681 (2022), DOI: 10.1016/j.enmm.2022.100681.
7) G. Divyapriya, S. Singh, C.A. Martínez-Huitle, J. Scaria, A.V. Karim, and P.V. Nidheesh, "Treatment of real wastewater by photoelectrochemical methods: An overview," *Chemosphere*, **130188** (2021), DOI: 10.1016/j.chemosphere.2021.130188.
8) S. Nayak, S.R. Prasad, D. Mandal, and P. Das, "Carbon dot cross-linked polyvinylpyrrolidone hybrid hydrogel for simultaneous dye adsorption, photodegradation and bacterial elimination from waste water," *Journal of hazardous materials*, **392**, 122287 (2020), https://doi.org/10.1016/j.jhazmat.2020.122287.
9) S. Ferhi, J. Vieillard, C. Garau, O. Poultier, L. Demey, R. Beaulieu, P. Penalva, V.Gobert and F.Portet-Koltalo, "Pilot-scale direct UV-C photodegradation of pesticides in groundwater and recycled wastewater for agricultural use," *Journal of Environmental Chemical Engineering*, **9**(5), 106120 (2021), DOI: 10.1016/J.JECE.2021.106120.
10) F. Taufany, M.J. Pasaribu, B.Y.S. Romaji, Y. Rahmawati, A. Altway, Susianto, S. Nurkhamidah, J.G. Anfias, Y. Mursidah, D. Fujanita, S. Yulianti, D. Rahmawati, and G. Stellarosari, "The Synthesis of Activated Carbon from Waste Tyre as Fuel Cell Catalyst Support," *EVERGREEN Joint Journal of Novel Carbon Resource Sciences & Green Asia Strategy*, **09**(02), 412-420 (2022), https://doi.org/10.5109/4794166.
11) P.P.D.K.Wulan, J.A. Ningtyas, and M. Hasanah, "The Effect of Nickel Coating on Stainless steel 316 on Growth of Carbon Nanotube from Polypropylene Waste," *EVERGREEN Joint Journal of Novel Carbon Resource Sciences & Green Asia Strategy*, **06** (01), 98-102 (2019), DOI: 10.5109/2328411.
12) N. Hamzah, M.F. Mohd Yasin, M.Z.M. Yusop, M.T. Zainal, and M.A.F. Rosli, "Identification of CNT Growth Region and Optimum Time for Catalyst Oxidation: Experimental and Modelling Studies of Flame Synthesis," *EVERGREEN Joint Journal of Novel Carbon Resource Sciences & Geen Asia Strategy*, **06** (01), 85-91(2019), https://doi.org/10.5109/2328409.
13) N. Talib, N.A. Jamaluddin, T.K. Sheng, L.W. Kiow, H. Abdullah, S. Ahmad, and A. Saleh, "Tribological Study of Activated Carbon Nanoparticle in Nonedible Nanofluid for Machining Application," *EVERGREEN Joint Journal of Novel Carbon Resource Sciences* & Green Asia Strategy, **08** (02), 454-460 (2021), https://doi.org/10.5109/4480728.
14) I.F. Andhika, T.E. Saraswati2, and S. Hastuti, "The Structural Characteristics of Carbon Nanoparticle Produced by Arc Discharge in Toluene Without Added Catalyst or Gases," *EVERGREEN Joint Journal of Novel Carbon Resource Sciences & Green Asia Strategy*, **07** (03), 417-428, (2020), https://doi.org/10.5109/4068622.
15) A.F. Ridassepri, F. Rahmawati, K.R. Heliani, Chairunnisa, J. Miyawaki, A.T. Wijayanta, "Activated Carbon from Bagasse and its Application for Water Vapor Adsorption," *EVERGREEN Joint Journal of Novel Carbon Resource Sciences & Green Asia Strategy*, **07** (03), 409-416, (2020), https://doi.org/10.5109/4068621.
16) N. Hashemi, and M. H. Mousazadeh, "Preparation of fluorescent nitrogen-doped carbon dots for highly selective on-off detection of Fe3+ ions in real samples," *Optical Materials*, **121**, 111515 (2021), https://doi.org/10.1016/j.optmat.2021.111515.

17) C. Wang, K. Yang, X. Wei, S. Ding, F. Tian, and F. Li, "One-pot solvothermal synthesis of carbon dots/Ag nanoparticles/TiO2 nanocomposites with enhanced photocatalytic performance," *Ceramics International*, **44**(18), 22481-22488 (2018), https://doi.org/10.1016/j.ceramint.2018.09.017.
18) S. Chahala, J. Macairan, N. Yousefi, N. Tufenkji and R. Naccache, "Green synthesis of carbon dots and their applications," RSC Adv., 11, 25354 (2021) DOI: 10.1039/D1RA04718C .
19) H. Yang, Y. Long, H. Li, S. Pan, H. Liu, J. Yang, and X. Hu, "Carbon dots synthesized by hydrothermal process via sodium citrate and NH4HCO3 for sensitive detection of temperature and sunset yellow," *Journal of colloid and interface science*, **516**, 192-201(2018), DOI: 10.1016/j.jcis.2018.01.054.
20) S. Kim, and J. Lauterbach, "Synthesis of ZSM-5 catalysts via microwave-assisted heating method for military jet fuel cracking into petroleum gas," *Microporous and Mesoporous Materials*, **328**, 111446 (2021), https://doi.org/10.1016/j.micromeso.2021.111446.
21) R. Sendão, M. D. V. M. de Yuso, M. Algarra, J. C. E. da Silva, and L. P. da Silva, "Comparative life cycle assessment of bottom-up synthesis routes for carbon dots derived from citric acid and urea," *Journal of Cleaner Production*, **254**, 120080 (2020), DOI: 10.1016/j.jclepro.2020.120080.
22) B. N. Jusuf, N. S. Sambudi, and S. Samsuri, "Microwave-assisted synthesis of carbon dots from eggshell membrane ashes by using sodium hydroxide and their usage for degradation of methylene blue," *Journal of environmental chemical engineering*, **6**(6), 7426-7433 (2018), https://doi.org/10.1016/j.jece.2018.10.032.
23) H. Gan, W. Han, Z. Fu, and L. Wang, "The chain-like Au/carbon dots nanocomposites with peroxidase-like activity and their application for glucose detection," *Colloids and Surfaces B: Biointerfaces*, **199**, 111553 (2021), https://doi.org/10.1016/j.colsurfb.2020.111553.
24) J. Ma, K. Li, S. Gu, Y. Wu, J. Zhang, J. Wu, L. Zhaoa and X. Lia, "Antimicrobial carbon-dot–stabilized silver nanoparticles", New J. Chem., **46**, 2546-2552 (2022), https://doi.org/10.1039/D1NJ05798G.
25) T. Feng, Q. Zeng, S. Lu, X. Yan, J. Liu, S. Tao, M. Yang, and B. Yang, "Color-tunable carbon dots possessing solid-state emission for full-color light-emitting diodes applications," *ACS Photonics*, **5**(2), 502-510 (2018), DOI:10.1021/ACSPHOTONICS.7B01010.
26) P. A. Putro, L. Roza and Isnaeni, "Photoluminescence Properties of Poly (Ethylene Glycol) Passivated Carbon Dots from Cassava Peels," *Indonesian Journal of Science and Education*, **3**(2) 76-81 (2019). doi: 10.31002/ijose.v3i2.1209
27) V. P. Sangeetha, S. Smriti, P. R. Solanki, and P. V. Mohanan, "Mechanism of action and cellular responses of HEK293 cells on challenge with zwitterionic carbon dots," *Colloids and Surfaces B: Biointerfaces*, **202**, 111698 (2021), https://doi.org/10.1016/j.colsurfb.2021.111698.
28) W. Ghann, V. Sharma, H. Kang, F. Karim, B. Richards, S.M. Mobin, J. Uddin, M.M. Rahman, F. Hossain, H. Kabir, and N. Uddin, "The synthesis and characterization of carbon dots and their application in dye sensitized solar cell," *International Journal of Hydrogen Energy*, **44**(29), 14580-14587 (2019), https://doi.org/10.1016/j.ijhydene.2019.04.072.
29) J. Gan, Y. Wu, F. Yang, H. Zhang, X. Wu, Y. Wang, and R. Xu, "Wood-cellulose photoluminescence material based on carbon quantum dot for light conversion," *Carbohydrate Polymers*, **290**, 119429 (2022), https://doi.org/10.1016/j.carbpol.2022.119429.
30) H. Li, Z. Kang, Y. Liu, and S. T. Lee, "Carbon nanodots: Synthesis, properties and applications," J. Mater. Chem. 22, 24230–24253 (2012). doi: 10.1039/c2jm34690g
31) Isnaeni, Y. Herbani, and M.M. Suliyanti, "Concentration effect on optical properties of carbon dots at room temperature," *Journal of Luminescence*, **198**, 215-219 (2018), https://doi.org/10.1016/j.jlumin.2018.02.012.
32) G.A.P.P. Sujana, M. Sumadiyasa, and I. Isnaeni, "Sintesis Carbon Dot Dengan Bahan Dasar Asam Sitrat Menggunakan Metode Pemanasan Secara Berulang di Dalam Oven Microwave," *BULETIN FISIKA*, **22**(1), 29-37 (2020).
33) B. Yin, H. Ma, S. Wang, and S. Chen, "Electrochemical synthesis of silver nanoparticles under protection of poly (N-vinylpyrrolidone)," *The Journal of Physical Chemistry B*, **107**(34), 8898-8904 (2003), https://doi.org/10.1021/jp001761r.
34) A. G. Zewudie, E. A. Zereffa*, T. A. Segne, H. C. A. Murthy, C. R. Ravikumar, D.Muniswamy, and B. B. Binagdie, "Biosynthesis of Ag/bentonite, ZnO/bentonite, and Ag/ZnO/bentonite nanocomposites by aqueous leaf extract of Hagenia abyssinica for antibacterial activities", REVIEWS ON ADVANCED MATERIALS SCIENCE, **62**(1) 20220307 (2023), https://doi.org/10.1515/rams-2022-030.
35) S. Darajat, H. Aziz, and A. Alif, "Seng Oksida (ZnO) sebagai fotokatalis pada proses degradasi senyawa biru metilene," *Jurnal Riset Kimia*, **1**(2), 179 (2015), https://doi.org/10.25077/jrk.v1i2.72.
36) M. P. Aji, P. A. Wiguna, N. Rosita, and S. Aisyah, "Carbon nanodots from frying oil as catalyst for photocatalytic degradation of methylene blue assisted solar light irradiation," *Am. J. Appl. Sci*, **13**(4), 432-438 (2016), https://doi.org/10.3844/ajassp.2016.432.438.

37) O. Bechambi, M. Chalbi, W. Najjar, and S. Sayadi, "Photocatalytic activity of ZnO doped with Ag on the degradation of endocrine disrupting under UV irradiation and the investigation of its antibacterial activity," *Applied Surface Science*, **347**, 414-420 (2015), https://doi.org/10.1016/j.apsusc.2015.03.049.
38) B. Jing, Z. Ao, W. Zhao, Y. Xu, Z. Chen, and T. An, "Evaluation procedure of photocatalysts for VOCs degradation from the view of density functional theory calculations: g-C3N4 dots/graphene as an example", *Journal of Materials Chemistry* A, **8**, 20363-20372 (2020), doi:10.1039/d0ta06060g.